

ON THE MISALIGNMENT BETWEEN CHROMOSPHERIC FEATURES AND THE MAGNETIC FIELD ON THE SUN

JUAN MARTÍNEZ-SYKORA^{1,2}, BART DE PONTIEU^{2,3}, MATS CARLSSON³, AND VIGGO HANSTEEN^{3,2}

¹ Bay Area Environmental Research Institute, Sonoma, CA 94952, USA

² Lockheed Martin Solar and Astrophysics Laboratory, Palo Alto, CA 94304, USA and

³ Institute of Theoretical Astrophysics, University of Oslo, P.O. Box 1029 Blindern, N-0315 Oslo, Norway

Draft version October 13, 2018

ABSTRACT

Observations of the upper chromosphere shows an enormous amount of intricate fine structure. Much of this comes in the form of linear features which are most often assumed to be well aligned with the direction of the magnetic field in the low plasma β regime thought to dominate the upper chromosphere. We use advanced radiative MHD simulations including the effects of ion-neutral interactions (using the generalized Ohm's law) in the partially ionized chromosphere to show that the magnetic field is often not well aligned with chromospheric features. This occurs where the ambipolar diffusion is large, i.e., ions and neutral populations decouple as the ion-neutral collision frequency drops, allowing the field to slip through the neutral population, currents perpendicular to the field are strong, and thermodynamic timescales are longer than or similar to those of ambipolar diffusion. We find this often happens in dynamic spicule or fibril-like features at the top of the chromosphere. This has important consequences for field extrapolation methods which increasingly use such upper chromospheric features to help constrain the chromospheric magnetic field: our results invalidate the underlying assumption that these features are aligned with the field. In addition, our results cast doubt on results from 1D hydrodynamic models, which assume that plasma remains on the same field lines. Finally, our simulations show that ambipolar diffusion significantly alters the amount of free energy available in the coronal part of our simulated volume, which is likely to have consequences for studies of flare initiation.

Subject headings: Magnetohydrodynamics (MHD) — Methods: numerical — Sun: atmosphere — Sun: magnetic topology

1. INTRODUCTION

Optically thick chromospheric spectral lines such as Ca II 8542Å or H α are formed over a wide range of heights from the photospheric line wings to the middle or upper chromosphere line core. Observations in these lines show a dramatic transition from wing features that appear to be dominated by convective motions or acoustic waves in the high plasma β regime (gas pressure is larger than magnetic pressure), to more linear features in the core of the lines that appear to trace magnetic field lines (e.g. Rouppe van der Voort et al. 2007; Cauzzi et al. 2008).

Because these linear features are most often assumed to reveal the direction of the magnetic field, chromospheric structuring is increasingly being used to help constrain magnetic field extrapolation codes (e.g. Wiegmann et al. 2008; Jing et al. 2011; Aschwanden 2016; Aschwanden et al. 2016; Zhu et al. 2016). Such codes typically use non-linear force-free field extrapolation methods based on photospheric magnetic field measurements. Since the boundary conditions are most readily measured in the photosphere but the field is not necessarily of a force-free nature at those heights, various methods are used to preprocess the magnetic field measurements (e.g. Régnier 2013) or to incorporate magnetic field information from a more force-free boundary region such as the upper chromosphere (Metcalf et al. 2008). The latter method is entirely dependent on the assumption that chromo-

spheric features such as fibrils and spicules, which dominate the upper chromosphere, are well aligned with the magnetic field. For example, Aschwanden et al. (2016) extrapolated magnetic field lines using photospheric vector field measurements from the Helioseismic Magnetic Imager (HMI, Scherrer et al. 2012) onboard of the Solar Dynamic Observatory (SDO, Pesnell et al. 2012) using the Vertical-Current Approximation Non-linear Force Free Field code (VAC-NLFFF code, Aschwanden 2016) which finds the best match of the extrapolated field lines with chromospheric and coronal features observed with the following imaging instruments: the Interferometric Bidimensional Spectrometre (IBIS, Cavallini 2006), the Rapid Oscillation in the Solar Atmosphere instrument (ROSA, Jess et al. 2010), the Interface Region Imaging Spectrograph (IRIS, De Pontieu et al. 2014), and Atmospheric Imager Assembly (AIA, Lemen et al. 2012) onboard of SDO.

Are these chromospheric structures really aligned with magnetic field lines? In the single-fluid MHD framework, the assumption that the upper chromosphere in the vicinity of network or plage is in the low plasma β regime and the observed features thus aligned with the magnetic field, seems reasonable. However, there are observational clues that this may not always be the case. For example, de la Cruz Rodríguez & Socas-Navarro (2011) show that in some cases chromospheric fibrils do not necessarily follow the magnetic field structures. They used Stokes profile observations of Ca II 8542 Å from the Spectro-Polarimeter for Infrared and

Optical Regions (SPINOR, Socas-Navarro et al. 2006) at the Dunn Solar Telescope and CRisp Imaging Spectro-Polarimeter (CRISP, Scharmer 2006) in full Stokes mode at the Swedish 1-m Solar Telescope (SST, Scharmer et al. 2003) and found that the misalignment of some fibrils with the magnetic field lines can be larger than 45 degrees.

What causes such a large deviation from the magnetic field direction? It is already known that, in principle, the neutral population in the partially ionized chromosphere can have an impact on the force-free nature of the chromospheric field (Arber et al. 2009). Is it possible that neutrals can also lead to misalignment of chromospheric features and the magnetic field?

In order to better understand this misalignment of the magnetic field lines with upper chromospheric features, we performed 2D advanced radiative MHD simulations using the *Bifrost* code (Gudiksen et al. 2011). We included the effects of the interaction between ions and neutrals in the magnetized and partially ionized gas of the middle to upper chromosphere by including ambipolar diffusion in the induction equation (the so-called generalized Ohm’s law) of our MHD code. Our simulations show that while neutrals are mostly coupled to the magnetic field through collisions with ions, under certain conditions the collisional frequency between neutrals and ions is low enough that the ions can become somewhat decoupled from the magnetic field, thereby allowing the magnetic field to diffuse and magnetic energy to be dissipated into thermal energy (see Cowling 1957; Braginskii 1965; Parker 2007, among others).

We find that our simulation naturally produces misalignment of the magnetic field and spicules. Our model thus provides an explanation for why some of the observations show field lines that are misaligned with chromospheric features, and which conditions can lead to such misalignment.

2. MODEL DESCRIPTION

The *Bifrost* code solves the full MHD equations with non-grey, non-LTE radiative transfer (Hayek et al. 2010; Carlsson & Leenaarts 2012) and thermal conduction along the magnetic field. The code is described in detail in Gudiksen et al. (2011). In addition, we have also included ion-neutral interaction effects adding two new terms to the induction equation, i.e., the Hall term and the ambipolar diffusion:

$$\frac{\partial \mathbf{B}}{\partial t} = \nabla \times [\mathbf{u} \times \mathbf{B} - \eta \mathbf{J} - \frac{\eta_{\text{Hall}}}{|B|} \mathbf{J} \times \mathbf{B} + \frac{\eta_{\text{amb}}}{B^2} (\mathbf{J} \times \mathbf{B}) \times \mathbf{B}] \quad (1)$$

where \mathbf{B} , \mathbf{J} , \mathbf{u} , and η , η_{Hall} , η_{amb} are the magnetic field, the current density, velocity field, the ohmic diffusion, the Hall term, and the ambipolar diffusion, respectively (see Cowling 1957; Braginskii 1965, for the derivation of this equation). Martínez-Sykora et al. (2016) describes the details of the implementation of the Hall term and ambipolar diffusion in the *Bifrost* code and extensive tests of this code are described by Martínez-Sykora et al. (2012). The collision cross sections used here are

the measurements and calculations listed by Vranjes & Krstic (2013).

For this work, it is relevant to reformulate expression 1 as follows:

$$\frac{\partial \mathbf{B}}{\partial t} = \nabla \times [\mathbf{u} \times \mathbf{B} - \eta \mathbf{J} - \mathbf{u}_{\text{H}} \times \mathbf{B} + \mathbf{u}_{\text{A}} \times \mathbf{B}] \quad (2)$$

where the Hall *velocity* is $\mathbf{u}_{\text{H}} = (\eta_{\text{Hall}} \mathbf{J})/|B|$ and the ambipolar *velocity* is $\mathbf{u}_{\text{A}} = (\eta_{\text{amb}} \mathbf{J} \times \mathbf{B})/B^2$ (see also Cheung & Cameron 2012; Martínez-Sykora et al. 2016). The ambipolar *velocity* can be understood as the velocity drift between ions and neutrals, i.e., the magnetic field lines are attached only to the ions. To gain a better intuitive grasp of how these effects (and *velocities*) act on the magnetic field, let us imagine a curved magnetic “field line” contained in a plane. Since the Hall velocity is a function of \mathbf{J} , the Hall velocity moves the magnetic field line out of the plane. Because the ambipolar diffusion is a function of $\mathbf{J} \times \mathbf{B}$, the ambipolar velocity will be perpendicular to the field line but contained within the plane. Therefore, the ambipolar diffusion relaxes the magnetic tension of the field line.

3. MODELS AND INITIAL CONDITIONS

The simulation used here is the so-called GOL (Generalized Ohm’s Law) simulation in Martínez-Sykora et al. (2016), i.e., it is a 2.5D model which spans from the upper layers of the convection zone (2.5 Mm below the photosphere) to the corona (40 Mm above the photosphere). Convective motions perform work on the magnetic field and introduce magnetic field stresses in the corona. This energy is dissipated and creates the corona self-consistently as the energy deposited by Joule heating is spread through thermal conduction (Gudiksen & Nordlund 2002) and the temperature reaches up to two million degrees (see top panel in Figure 1). The horizontal domain spans 96 Mm. The spatial resolution is uniform along the horizontal axis (14 km) and non-uniform in the vertical axis allowing smaller grid size where needed, i.e., in locations such as the photosphere and the transition region (~ 12 km).

The initial magnetic field has two plage regions of opposite polarity that are connected and form loops that are up to ~ 50 Mm long (Figure 1). The mean unsigned field strength at the photosphere is ~ 190 G. The initial magnetic field is a potential field. First we run this setup for roughly 1.5 hours. After transients have passed through the domain, we continue the simulation for another half hour of solar time (see Martínez-Sykora et al. 2016, for a detailed description of the setup of the model).

4. RESULTS

The ion-neutral interaction effects implemented through the generalized Ohm’s law, strongly influence the state of the simulated chromosphere (Martínez-Sykora et al. 2016). Here, we focus on misalignment of the magnetic field direction from the chromospheric thermodynamic features.

Generally, the ion-neutral interaction effects impact the magnetic field distribution and configuration. In

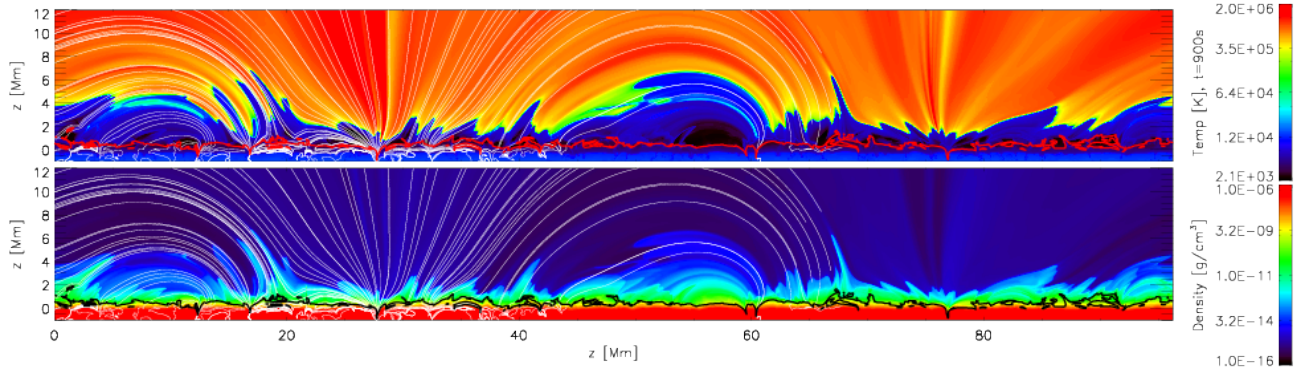


FIG. 1.— Temperature map (top panel) and density map (bottom panel) are shown in logarithmic scale. Magnetic field lines are drawn in the left hand side of the maps and plasma beta unity is the thick contour (red in the top panel and black in the bottom panel).

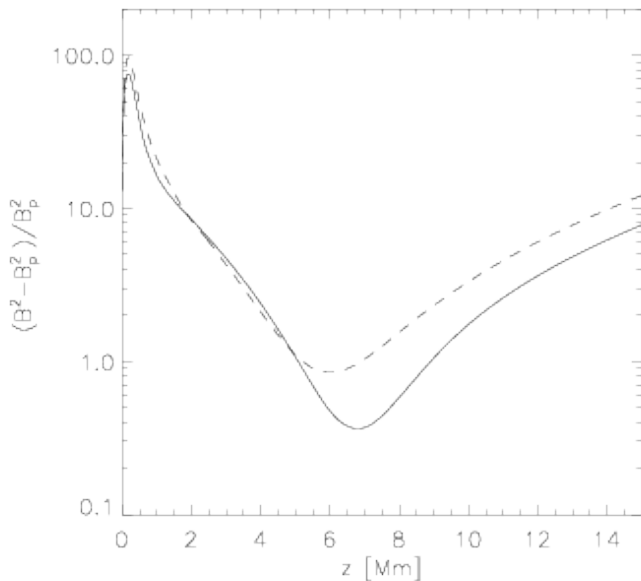


FIG. 2.— Magnetic free energy, normalized by the magnetic energy of the potential field extrapolated from $z=0$ Mm and integrated over 20 minutes, for the simulation that includes ion-neutral interaction effects (solid) and for the equivalent simulation which does not include ion-neutral interaction effects (dashed).

Figure 2 we compare the magnetic free energy from the model that includes ion-neutral interaction effects with the free energy in an equivalent model which has been run without ion-neutral interaction effects. The ambipolar diffusion helps to accumulate a bit of extra magnetic free energy in the middle-upper chromosphere and transition region but reduces it in photosphere (10%) and a factor between 1.5 and 4 in the corona. The magnetic free energy is reduced in the photosphere because a small portion of the accumulated magnetic field in the photosphere is sporadically diffused into the chromosphere in regions where the ambipolar diffusion is large enough at low enough heights (Martínez-Sykora et al. 2016). Ion-neutral interaction effects prevent magnetic free energy from reaching the corona because it is largely dissipated in the chromosphere due to the ambipolar diffusion.

We also find that, under certain chromospheric conditions, thermodynamic structures may decouple from the magnetic field lines due to the ambipolar *velocity*. As a result of this, the simulation shows some spicules and

other chromospheric features misaligned from the magnetic field during their evolution. Figure 3 shows temperature maps of the evolution of several spicules with magnetic field lines overplotted as white lines. At the early stages of spicule evolution, they follow the magnetic field lines. However, as the spicules evolve in time, field lines start to decouple from the apparent spicular structure. This figure shows misalignment angles of up to 25 degrees, and this simulation shows features that can reach a misalignment with field lines of up to 40 degrees in the most extreme cases. As a result, sometimes, the magnetic field lines do not follow the thermal structures in the upper chromosphere and transition region.

This also impacts the evolution of the features. Towards the end of the evolution of these spicules, they become wider and their footpoints drift from left to right.

The thermodynamic chromospheric features do not follow the magnetic field lines when the following conditions are met: 1) ambipolar diffusion, magnetic field strength and the current perpendicular to the magnetic field are high enough; 2) the timescales of the thermodynamic processes are longer than, or of the same order as the ambipolar timescales.

This often occurs in upper chromospheric spicules for several reasons. Since the density drops drastically as a function of height and also as a function of time (because of the expansion of the spicule), the ambipolar diffusion increases drastically (panel C, Figure 4). This is a result of low temperature and low ion-neutral collision frequency.

One component of the magnetic field *advection* comes from the ambipolar velocity (Panel B) which differs from the advection flows and the direction of the spicule and separate the magnetic field lines from the spicule. Consequently, the field lines along the spicule have two velocity components: 1) one from the advection which is the same as the plasma motion (Equation 2), i.e., this flow will move the field lines and the chromospheric features in the same direction (see the flow velocity in Panel A in Figure 4), 2) and the second component which is completely detached from the plasma motion and perpendicular to the field lines (see the ambipolar *velocity* in Panel B in Figure 4). The latter component is the one that leads to a misalignment of the field lines with the spicules. This misalignment is large as long as the displacement of the field lines due to the ambipolar *velocity* is large enough during the lifetime of the spicule.

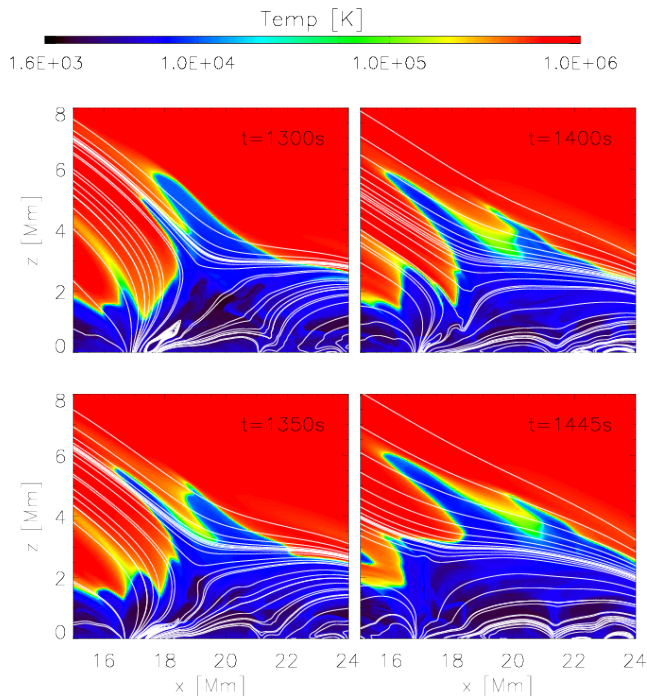


FIG. 3.— Temperature maps in logarithmic scale at $t=1260s$ (top-left), $1350s$ (bottom-left), $1445s$ (top-right) and $1540s$ (bottom-right) with magnetic field lines shown in white. At the beginning (left panels), the thermodynamic structures are aligned with the magnetic field, whereas at later times (right panels) the magnetic connectivity has changed and the alignment is poor.

5. DISCUSSION

Our 2.5D radiative MHD simulation includes ion-neutral interaction effects and produces some examples of chromospheric features that are decoupled from the magnetic field direction. This is a result of ion-neutral interaction effects in the chromosphere and can occur when the ambipolar diffusion and the current perpendicular to the magnetic field lines are large, and the thermo-dynamic timescales are at least of the same order as the ambipolar velocity timescales. The simulated features that become misaligned from the magnetic field have lifetimes of order a few minutes. The time-scale becomes shorter in regions with large currents perpendicular to the magnetic field lines and large ambipolar diffusion due to low values of the temperature, ion-neutral collision frequency and/or ionization degree. Under these conditions the magnetic field may undergo evolution that is different from that of the thermodynamic structures. For example, decaying spicules may change their connectivity with “different” field lines crossing the spicule. In such a case, instead of following a space-time parabolic profile along a fixed direction, the spicule may show a horizontal displacement at the same time as they disappear (towards the end of their lifetime). This process can provide a natural explanation for the observations of de la Cruz Rodríguez & Socas-Navarro (2011) where fibrils or spicule-like features do not necessarily follow the magnetic field direction.

Our model shows that the misalignment is not uniform in space or time, with some structures less affected. In addition, dynamic features appear to be typically more

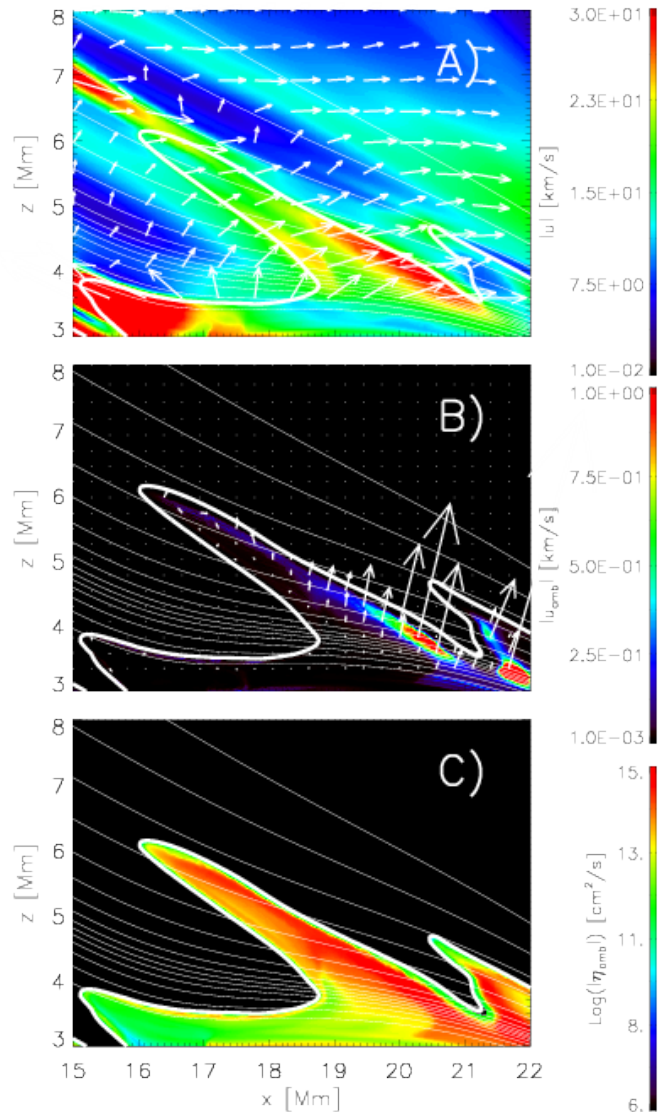


FIG. 4.— Absolute velocity map with velocity field as white vectors are shown in panel A, absolute ambipolar *velocity* map with ambipolar *velocity* field as white vectors are shown in panel B, and the ambipolar diffusion in logarithmic scale is shown in panel C. Magnetic field lines are shown as thin white lines and the temperature contour at 10^5 K is shown with a thick white line.

misaligned towards the end of their lifetime. This occurs in particular in regions with enough current perpendicular to the magnetic field, i.e., where there is large magnetic tension. Such conditions can also be expected in active regions with strong currents, such as in newly emerging active regions. However, it is a priori not clear how one can determine from the observations alone which features are likely not well aligned with the magnetic field. Future work will be needed to investigate how misalignment can be estimated based on observational clues, such as the temporal behavior of the structures or the presence of currents.

Our results suggest that ion-neutral interaction effects may have a significant impact on magnetic field extrapolation methods. Within the chromosphere, the ambipolar diffusion shows strong variations in both space and time. In regions where the ambipolar diffusion is

strong the magnetic field will be more potential. However, at the boundaries between regions of strong and weak ambipolar diffusion, the magnetic field lines may have strong changes in the connectivity. These variations in space and time of the ambipolar diffusion impact the magneto-thermodynamic processes in the chromosphere (Martínez-Sykora et al. 2016). This was missing in previous numerical models (Carlsson et al. 2016). It is unclear how such spatial and temporal complexity can be captured in field extrapolation methods that are based on photospheric vector magnetograms.

In addition, magnetic field extrapolation codes that attempt to use the direction of chromospheric features in order to find the best match with the field lines may provide field configurations that are incorrect. This is because the magnetic field may not be well aligned with the chromospheric features due to the presence of ambipolar diffusion. As a result of this, the measurements of the misalignment between features and magnetic field extrapolation using these methods may be incorrect and in general underestimated (Aschwanden et al. 2016). Future studies of these extrapolation codes should investigate this issue further by trying the method on synthetic data from this type of radiative MHD models that include ion-neutral interaction effects and comparing with the actual magnetic field.

Many studies of the solar atmosphere, in particular the corona, are undertaken using 1D hydrodynamic loop models (e.g. Klimchuk & Bradshaw 2014). Such models are based on the assumption that the thermodynamic evolution occurs along magnetic field lines or tubes (1D). However, our results indicate that decoupling of the field lines from plasma is a frequent occurrence in the chromosphere. This will change the connectivity of each element along the 1D models. In addition, ambipolar diffusion fundamentally undermines the assumption that the plasma is tied to the field on timescales of many minutes. As we have shown, this is not always the case. Therefore, these 1D models cannot capture or mimic the physics of the processes that connect the corona to the chromosphere and transition region.

Leake & Arber (2006) performed 2D simulations of flux emergence with ambipolar diffusion. They also notice that the magnetic field is more potential in the atmosphere due to the ambipolar dissipation. However, they get several orders of magnitude smaller currents for the case with ambipolar diffusion than without ambipolar diffusion whereas we get from 1.5 to 4 times smaller in the case for ambipolar diffusion than without ambipolar diffusion. This is most likely due to the highly simplified setup of the ambipolar diffusion in their model chromo-

sphere and also due to their missing many of the chromospheric processes driven by the convective motion.

Our results also have a potential impact on more advanced 3D radiative MHD models. This is because the magnetic field energy deposition in the corona in radiative MHD models will change as soon as ion-neutral interaction effects are introduced. For example, Peter (2015) noticed that larger domains show stronger flows and Doppler shifts for transition region EUV profiles (similar to observations) compared to smaller simulated domains (Hansteen et al. 2010, 2015). Ion-neutral interaction effects will impact these results and deeper investigations that include ion-neutral effects must be performed for computational domains of various sizes.

Our simulation suffers from several limitations that need to be addressed. Our simulation does not include time dependent ionization which will impact the spatial and temporal distribution of ambipolar diffusion in the chromosphere (Leenaarts et al. 2007; Golding et al. 2014). The process described above is also strongly constrained to the two dimensions of the model, therefore the expansion of these models into three dimensions is needed. Finally, the Generalized Ohm's law is valid as long as the time scales are much larger than the ion-neutral collision frequencies, but in the transition region this may not always be fulfilled and ions may decouple from neutrals (Martínez-Sykora et al. 2012). This can potentially alter these results.

6. ACKNOWLEDGMENTS

We gratefully acknowledge support by NASA grants NNX11AN98G, NNM12AB40P, NNH15ZDA001N-HSR, NNX16AG90G, and NASA contracts NNM07AA01C (Hinode), and NNG09FA40C (IRIS). This research was supported by the Research Council of Norway and by the European Research Council under the European Union's Seventh Framework Programme (FP7/2007-2013) / ERC Grant agreement nr. 291058. The simulations have been run on clusters from the Notur project, and the Pleiades cluster through the computing project s1061 from the High End Computing (HEC) division of NASA. We thankfully acknowledge the computer and super-computer resources of the Research Council of Norway through grant 170935/V30 and through grants of computing time from the Programme for Supercomputing. This work has benefited from discussions at the International Space Science Institute (ISSI) meetings on "Heating of the magnetized chromosphere" where many aspects of this paper were discussed with other colleagues. To analyze the data we have used IDL.

REFERENCES

- Arber T. D., Botha G. J. J., Brady C. S., 2009, *ApJ*, 705, 1183, Effect of Solar Chromospheric Neutrals on Equilibrium Field Structures
- Aschwanden M. J., 2016, ArXiv e-prints, The Vertical Current Approximation Nonlinear Force-Free Field Code - Description, Performance Tests, and Measurements of Magnetic Energies Dissipated in Solar Flares
- Aschwanden M. J., Reardon K., Jess D., 2016, ArXiv e-prints, Tracing the Chromospheric and Coronal Magnetic Field with AIA, IRIS, IBIS, and ROSA Data
- Braginskii S. I., 1965, *Reviews of Plasma Physics*, 1, 205, Transport Processes in a Plasma
- Carlsson M., Hansteen V. H., Gudiksen B. V., Leenaarts J., De Pontieu B., 2016, *A&A*, 585, A4, A publicly available simulation of an enhanced network region of the Sun
- Carlsson M., Leenaarts J., 2012, *A&A*, 539, A39, Approximations for radiative cooling and heating in the solar chromosphere
- Cauzzi G., Reardon K. P., Uitenbroek H., et al., 2008, *A&A*, 480, 515, The solar chromosphere at high resolution with IBIS. I. New insights from the Ca II 854.2 nm line
- Cavallini F., 2006, *Sol. Phys.*, 236, 415, IBIS: A New Post-Focus Instrument for Solar Imaging Spectroscopy
- Cheung M. C. M., Cameron R. H., 2012, *ApJ*, 750, 6, Magnetohydrodynamics of the Weakly Ionized Solar Photosphere

- Cowling T. G., 1957, *Magnetohydrodynamics. Interscience tracts on physics and astronomy*
- de la Cruz Rodríguez J., Socas-Navarro H., 2011, *A&A*, 527, L8, Are solar chromospheric fibrils tracing the magnetic field?
- De Pontieu B., Title A. M., Lemen J. R., et al., 2014, *Sol. Phys.*, The Interface Region Imaging Spectrograph (IRIS)
- Golding T. P., Carlsson M., Leenaarts J., 2014, *ApJ*, 784, 30, Detailed and Simplified Nonequilibrium Helium Ionization in the Solar Atmosphere
- Gudiksen B. V., Carlsson M., Hansteen V. H., et al., 2011, *A&A*, 531, A154, The stellar atmosphere simulation code Bifrost. Code description and validation
- Gudiksen B. V., Nordlund Å., 2002, *ApJ*, 572, L113, Bulk Heating and Slender Magnetic Loops in the Solar Corona
- Hansteen V., Guerreiro N., De Pontieu B., Carlsson M., 2015, *ApJ*, 811, 106, Numerical Simulations of Coronal Heating through Footpoint Braiding
- Hansteen V. H., Hara H., De Pontieu B., Carlsson M., 2010, *ApJ*, 718, 1070, On Redshifts and Blueshifts in the Transition Region and Corona
- Hayek W., Asplund M., Carlsson M., et al., 2010, *A&A*, 517, A49, Radiative transfer with scattering for domain-decomposed 3D MHD simulations of cool stellar atmospheres. Numerical methods and application to the quiet, non-magnetic, surface of a solar-type star
- Jess D. B., Mathioudakis M., Christian D. J., et al., 2010, *Sol. Phys.*, 261, 363, ROSA: A High-cadence, Synchronized Multi-camera Solar Imaging System
- Jing J., Yuan Y., Reardon K., et al., 2011, *ApJ*, 739, 67, Nonpotentiality of Chromospheric Fibrils in NOAA Active Regions 11092 and 9661
- Klimchuk J. A., Bradshaw S. J., 2014, *ApJ*, 791, 60, Are Chromospheric Nanoflares a Primary Source of Coronal Plasma?
- Leake J. E., Arber T. D., 2006, *A&A*, 450, 805, The emergence of magnetic flux through a partially ionised solar atmosphere
- Leenaarts J., Carlsson M., Hansteen V., Rutten R. J., 2007, *A&A*, 473, 625, Non-equilibrium hydrogen ionization in 2D simulations of the solar atmosphere
- Lemen J. R., Title A. M., Akin D. J., et al., 2012, *Sol. Phys.*, 275, 17, The Atmospheric Imaging Assembly (AIA) on the Solar Dynamics Observatory (SDO)
- Martínez-Sykora J., De Pontieu B., Hansteen V., 2012, *ApJ*, 753, 161, Two-dimensional Radiative Magnetohydrodynamic Simulations of the Importance of Partial Ionization in the Chromosphere
- Martínez-Sykora J., De Pontieu B., Hansteen V., et al., 2016, *ApJ*, in prep, Two-dimensional Radiative Magnetohydrodynamic Simulations of the Importance of Partial Ionization in the Chromosphere. II. Impact on the solar atmosphere
- Metcalf T. R., De Rosa M. L., Schrijver C. J., et al., 2008, *Sol. Phys.*, 247, 269, Nonlinear Force-Free Modeling of Coronal Magnetic Fields. II. Modeling a Filament Arcade and Simulated Chromospheric and Photospheric Vector Fields
- Parker E. N., 2007, *Conversations on Electric and Magnetic Fields in the Cosmos*. Princeton University Press
- Pesnell W. D., Thompson B. J., Chamberlin P. C., 2012, *Sol. Phys.*, 275, 3, The Solar Dynamics Observatory (SDO)
- Peter H., 2015, *Philosophical Transactions of the Royal Society of London Series A*, 373, 20150055, What can large-scale magnetohydrodynamic numerical experiments tell us about coronal heating?
- Régnier S., 2013, *Sol. Phys.*, 288, 481, Magnetic Field Extrapolations into the Corona: Success and Future Improvements
- Roupe van der Voort L. H. M., De Pontieu B., Hansteen V. H., Carlsson M., van Noort M., 2007, *ApJ*, 660, L169, Magnetoacoustic Shocks as a Driver of Quiet-Sun Mottles
- Scharmer G. B., 2006, *A&A*, 447, 1111, Comments on the optimization of high resolution Fabry-Pérot filtergraphs
- Scharmer G. B., Bjelksjo K., Korhonen T. K., Lindberg B., Petterson B., 2003, *The 1-meter Swedish solar telescope*, en *Society of Photo-Optical Instrumentation Engineers (SPIE) Conference Series*, Vol. 4853, Keil S. L., Avakyan S. V. (eds.), *Society of Photo-Optical Instrumentation Engineers (SPIE) Conference Series*, p. 341
- Scherrer P. H., Schou J., Bush R. I., et al., 2012, *Sol. Phys.*, 275, 207, The Helioseismic and Magnetic Imager (HMI) Investigation for the Solar Dynamics Observatory (SDO)
- Socas-Navarro H., Elmore D., Pietarila A., et al., 2006, *Sol. Phys.*, 235, 55, Spinor: Visible and Infrared Spectro-Polarimetry at the National Solar Observatory
- Vranjes J., Krstic P. S., 2013, *A&A*, 554, A22, Collisions, magnetization, and transport coefficients in the lower solar atmosphere
- Wiegmann T., Thalmann J. K., Schrijver C. J., De Rosa M. L., Metcalf T. R., 2008, *Sol. Phys.*, 247, 249, Can We Improve the Preprocessing of Photospheric Vector Magnetograms by the Inclusion of Chromospheric Observations?
- Zhu X., Wang H., Du Z., He H., 2016, *ArXiv e-prints*, Forced field extrapolation of the magnetic structure of the H α fibrils in solar chromosphere